Desalination and Water Treatment
www.deswater.com

doi: 10.5004/dwt.2019.23746

152 (2019) 197–207
June

Modification of SiO_2 by n-dodecyltrimethoxysilane and preparation of SiO_2-filled regenerated cellulose nanocomposite membranes for dehydration of caprolactam by pervaporation

Siqian Hu[a], Zaikun Wu[b], Zhihua Xu[a], Tianrong Zhu[a,*]

[a]*Key Laboratory of Optoelectronic Chemical Materials and Devices (Jianghan University), Ministry of Education, Jianghan University, Wuhan 430072, China, Tel. +86-27-84226806; Fax: +86-27-84226806; email: zhutiarnong@whu.edu.cn (T. Zhu)*
[b]*Key Laboratory of Green Chemical Process of Ministry of Education, Key Laboratory of Novel Reactor and Green Chemical Technology of Hubei Province, School of Chemical Engineering & Pharmacy, Wuhan Institute of Technology, Wuhan 430073, China*

Received 9 July 208; Accepted 2 January 2019

ABSTRACT

Novel organic–inorganic nanocomposite pervaporation membranes were prepared by the incorporation of the unmodified and modified SiO_2 nanoparticles with a silane coupling agent (WD10, $C_{12}H_{25}Si(OCH_3)_3$) into regenerated cellulose (RC) membranes. The WD10-modified SiO_2 particles were characterized by FTIR. The chemical and physical properties of the membranes were characterized by attenuated total reflection-Fourier transform infrared, AFM, scanning electron microscopy, thermogravimetric analysis, XRD and degree of swelling measurements. Furthermore, the effects of nano-SiO_2, WD10-modified SiO_2, WD10, feed temperature and feed concentration on the pervaporation performances were investigated for caprolactam dehydration by pervaporation. Among all the prepared membranes, RC-SiO_2 (5%)-WD10 nanocomposite membrane exhibited excellent pervaporation (PV) properties with a flux of 611.3 g m^{-2} h^{-1} and separation factor of 95,404.8 at 333 K, for 70 wt.% caprolactam. Diffusion coefficient of water and caprolactam molecules was analyzed by Fick's equation. The results show that the diffusion plays a dominant role in the transport of binary liquid molecules in PV process. The membranes developed in the present study have the ability for the separation of caprolactam–water mixture.

Keywords: Regenerated cellulose; Pervaporation; SiO_2; WD10; Caprolactam–water

1. Introduction

Membrane technology is a promising separation method which has been widely used in industrial processes due to an energy-efficient alternative to distillation, easy operation and high-energy savings [1]. Pervaporation (PV) is one of the membrane processes, which is attracted considerable attention currently because it can be operated at lower temperatures than other separation methods [2]. Over the past several decades, PV has been widely studied for separation aqueous–organic azeotropes, closely boiling mixtures, isomers, as well as being safe to handle the heat-sensitive compounds [3]. Caprolactam ($C_6H_{11}NO$) is synthesized via the cyclohexanone oximation and Beckmann rearrangement route using highly concentrated sulfuric acid and neutralizing the reaction mixture with aqueous ammonia which is a very heat-sensitive substance [2,3]. Water is the most important impurity in the final caprolactam purification because the existence of water can hinder the growth of molecular weight [2,4]. To prevent decomposition, distillation through triple-effect evaporation sets, crystallization under a reduced pressure and melt crystallization by suspension

---

* Corresponding author.

1944-3994/1944-3986

are usually used for the purification in recent years [5]. But these processes suffer from high energy consumption, high operating costs and the pollutants being transferred to a second phase. Therefore, it is necessary to develop a new dehydration process for the concentrate of caprolactam–water mixtures. So its purification by PV has been studied by Zhang et al. [6–8].

As for caprolactam–water mixtures, the molecular size of water is smaller than caprolactam. Furthermore, water is more hydrophilic and polar than caprolactam due to dipole moment of hydroxyl group. So water is both preferentially transported and sorped in the hydrophilic membranes. Accordingly, the molecular size and polarity difference should be a key factor to obtain a higher permselectivity [9]. Cellulose is considered as being the most abundant polysaccharide available worldwide and an almost inexhaustible source of raw material for the increasing demand for environmentally friendly products [2,10]. Regenerated cellulose (RC) membranes, prepared from cellulose in NaOH/urea aqueous solution by the phase inversion method, have been widely applied to membrane separation techniques such as dialysis, ultrafiltration and purification of mixtures, due to hydrophilicity, solute permeability and solvent resistant [2]. The RC membrane exhibits a high hydrophilicity, so it is a good candidate for pervaporation [2]. This membrane with higher permeation flux was used in pervaporation for separation of ethanol–water mixtures [1,11]. So the RC membrane is a good choice for PV dehydration of caprolactam. However, the wide application of RC membrane is limited by lack of good separation factor. Inorganic-polymer hybrid membranes have the synergistic to combine the desired properties of organic and inorganic systems [12,13], so they have attracted considerable attention as potential "next generation" membrane materials [14].

SiO_2 is the hydrophilic inorganic material because it has a large number of silanol and siloxane groups on the surface making it highly polar, which is able to uptake water more strongly. So it will improve the RC membrane properties with higher water uptake and better PV performances. Polymer/SiO_2 nanocomposite membranes are typically prepared by solution-casting mixtures of nano-SiO_2 and polymer, and such membranes have received much attention in the past decade [15–18]. The dispersion of nanosized particles in the polymer matrix has an important impact on the properties of membranes. A good dispersion may be realized by surface chemical modification of the nanoparticles [15]. Coupling agents can help to improve the compatibility between polymer matrix and nano-SiO_2. Zhou et al. [19] used a silane coupling agent, vinyltrimethoxysilane, to modify the surface of silicalite-1 to improve the compatibility between PDMS and silicalite-1, and found that a higher selectivity was obtained with hybrid membrane. Peng et al. [20] used a silane coupling agent, $NH_2–C_3H_6–Si(OC_2H_5)_3$, to modify the surface of nano-fumed silica particles, and found that the pervaporation performances of the composite membranes were improved by adding the modified silica particles significantly.

In this paper, novel organic–inorganic nanocomposite pervaporation membranes were prepared by the incorporation of the unmodified or modified SiO_2 nanoparticles with a silane coupling agent (WD10, $C_{12}H_{25}Si(OCH_3)_3$) into RC membranes. The aim of the presented work was to investigate the feasibility of preparing high performance pervaporation membranes by incorporating unmodified SiO_2 or WD10-modified SiO_2 into RC membrane. A 5 wt.% WD10 solution was also directly added into cellulose-unmodified SiO_2 polymer mixture solution for the crosslinking reaction. The modified SiO_2 was analyzed by FTIR. The morphology, crystalline structure and thermal stability of the membranes were characterized in detail. The effects of nano-SiO_2, WD10-modified SiO_2, WD10, feed temperature and feed concentration on the pervaporation performances of the nanocomposite RC membranes were examined for caprolactam dehydration by pervaporation.

2. Experimental

2.1. Materials

The cellulose (cotton linter pulp, α-cellulose content > 95%) was provided by Hubei Chemical Fiber Group Ltd. (Xiangfan, China). The cotton linter pulp was shattered and dried for 8 h in a vacuum oven. Nano-silica (SiO_2) (20 nm) and silane coupling reagent (WD10, $C_{12}H_{25}Si(OCH_3)_3$) were purchased from Hubei Wuhan University Silicone New Material Co., Ltd., China. Caprolactam (chemical pure) was purchased by Baling Petrochemical Co. Ltd. (SINOPEC, China).

2.2. Modification of SiO_2 nanoparticles

The SiO_2 nanoparticle surface was modified in the silane coupling agent (WD10) toluene solution and the reaction mixture was stirred at 70°C for 6 h. The precipitate was then centrifuged and subjected to repeat centrifugal washing with menthol to remove completely the unreacted WD10. The white powder was finally obtained by drying in a vacuum oven at 60°C.

2.3. Preparation of SiO_2-filled RC membranes

The SiO_2-RC composite membranes were prepared by the phase inversion method. First, formulation of cellulose solution, an amount of 3.2 g of cotton linter was added in 76.8 g of 7 wt.% NaOH/12 wt.% urea aqueous solvents (−12°C) with vigorous stirring to obtain a homogeneous solution according to a study by Song et al. [21]. Second, the SiO_2, surface modified SiO_2 nanoparticles or WD10 were added into the cellulose coating solution and stirring in order to obtain optimal particle dispersion. The solution was then centrifuged to remove the bubble. The composition of the casting solution is exhibited in Table 1. The solutions were converted into the nonporous structure of RC membrane by the method as described in a study by Zhu et al. [2].

2.4. Characterization of membranes

Membrane surface roughness was investigated by AFM analysis (SPM-9500J3, Shimadzu, Kyoto, Japan). The analysis method was used as described in the study by Zhu et al. [2]. In addition, the surface of the membrane was analyzed by

Table 1
Composition of casting solutions

Membrane	Cellulose (wt.%)	Solution* (wt.%)	SiO_2 (by weight of cellulose, wt.%)	Modified SiO_2 (by weight of cellulose, wt.%)	WD10 (by weight of SiO_2, wt.%)	Appearance of the membranes
RC-0	4	96	0	0	0	Transparent
RC-SiO_2 (5%)	4	96	5	0	0	Transparent
RC-SiO_2 (10%)	4	96	10	0	0	Transparent
RC-modified SiO_2 (5%)	4	96	0	5	0	Transparent
RC-SiO_2 (5%)-WD10	4	96	0	5	5	Transparent

*7 wt.% NaOH–12 wt.% urea aqueous solution.

using a scanning electron microscopy (SEM) (FEI Quanta 200, Holland).

In order to understand the surface functional groups of nanocomposite membrane, the membrane surface was characterized by the attenuated total reflection-Fourier transform infrared (ATR-FTIR) spectra, which were performed by using the Nicolet iS10 FTIR spectrophotometer. FTIR spectra were recorded within the range of 4,000–500 cm^{-1}.

The XRD patterns of the membrane samples were determined by a D8 Advance X-ray diffractometer (Bruker, Germany) using Cu Kα radiation with the angle of diffraction varying from 8° to 40°.

The thermal stability of the nanocomposite membrane was analyzed with Setaram SETSYS Evolution 16 thermogravimetric analyzer by heating from room temperature to 600°C at a rate of 10°C min^{-1} under nitrogen gas.

2.5. Swelling experiments

The swelling experiment was analyzed as given in a study by Zhu et al. [3]. All experiments were repeated at least three times. The results were averaged.

The degree of swelling (DS, %) was calculated as follows:

$$\text{DS}\left(\%\right) = \frac{W_s - W_d}{W_d} \times 100\% \tag{1}$$

where W_d and W_s were the weights of the dried and swollen membranes, respectively.

2.6. Pervaporation experiments

The experimental pervaporation setup and method were used according to the study by Zhu et al. [2,3]. To determine the composition of permeate by high performance liquid chromatography (HPLC), samples were passed through a 0.22 mm filter and submitted for analysis. HPLC was performed on a reverse phase C18 column (150 mm × 4.6 mm, Shimadzu, Japan) with a methanol/water (50:50, v/v) mobile phase at a flow rate of 0.5 mL min^{-1}. Detection was performed with a UV detector (SPD-10A, Shimadzu, Japan). Analysis was performed at 230 nm for caprolactam. The compositions of the liquid feed mixtures were analyzed by measuring the refractive index within an accuracy of ±0.0001 units using high-precision Abbe Refractometer (Atago NAR-3T, Japan), which can be calculated by using previously established standard graph of refractive index vs. known mixture composition. The refractometer prism was maintained at 25°C ± 0.1°C [3].

The permeation flux (J, g m^{-2} h^{-1}) was defined as follows:

$$J\left(\text{gm}^{-2}\text{h}^{-1}\right) = \frac{W\left(g\right)}{A\left(\text{m}^2\right) \times t\left(h\right)} \tag{2}$$

where W is the weight of penetrant, A is the effective membrane area and t is the measuring time.

The separation factor α was calculated as follows:

$$\alpha = \frac{y_{\text{water}} / y_{\text{caprolactam}}}{x_{\text{water}} / x_{\text{caprolactam}}} \tag{3}$$

where x_{water}, $x_{\text{caprolactam}}$ and y_{water}, $y_{\text{caprolactam}}$ are the mole fraction of water and caprolactam in the feed and permeate, respectively.

Permeance and membrane selectivity were used to clarify the contribution by the nature of the membrane to separation performance. The basic transport equation for pervaporation can be written as follows [22]:

$$J_i = \frac{\left(D_i S_i\right)}{\delta\left(p_{i,\text{feed}} - p_{i,\text{permeate}}\right)} = Q_i\left(p_{i,\text{feed}} - p_{i,\text{permeate}}\right) \tag{4}$$

On the basis of Raoult's law (feed side) and Dalton's law (permeate side) it is equal:

$$J_i = Q_i\left(x_i \gamma_i p^{\text{o}}_{i,\text{feed}} - y_i p_{\text{permeate}}\right) \tag{5}$$

where J_i is the permeation flux, Q_i is the permeance of the membrane for i (which equals the permeability coefficient divided by the membrane thickness), x_i, y_i are the mole fraction of i in the feed and the permeate, respectively, γ_i is the activity coefficient of i in the feed liquid and $p^{\text{o}}_{i,\text{feed}}$ is the saturation vapor pressure of pure i in the feed liquid temperature, p_{permeate} is the permeate pressure.

The membrane selectivity (α_{mem}) is an intrinsic property of the membrane material, which is defined as the ratio of the water permeance over the caprolactam permeance.

$$\alpha_{\text{membane}} = \frac{Q_{\text{water}}}{Q_{\text{caprolactam}}} \tag{6}$$

3. Results and discussion

3.1. FTIR of WD10-modified SiO_2 nanoparticles

The WD10-modified SiO_2 nanoparticles were characterized by FTIR (Fig. 1). The peaks of organic C–H were observed in the 2,800–3,000 cm^{-1} regions, indicating the coupling agent WD10 was successfully grafted on the surface of SiO_2. The characteristic absorption band of Si–O–Si asymmetric stretching (1,100 cm^{-1}) became stronger by adding the coupling agent, indicating a more "condensed" silica network [15].

3.2. Membrane characterization

The solutions of cellulose-SiO_2, cellulose-modified SiO_2 and their blend with WD10 were optically colorless and transparent. No phase separation or precipitation was observed even after centrifugation. Fig. 2 represents interaction between (1) cellulose and SiO_2, (2) WD10 and SiO_2, and (3,4) the crosslinking mechanism of cellulose with WD10. The interaction between cellulose and SiO_2 suggested the formation of covalent bonds due to etherification of cellulose hydroxyl groups on silanol groups of silica network.

3.2.1. ATR-FTIR analysis

Fig. 3 presents the ATR-FTIR spectra of pure RC and its nanocomposite with SiO_2 particles and silane coupling reagent (WD10). With SiO_2 content increased from 5 to 10 wt.%, the 3,330 cm^{-1} peak (–OH) enhanced and the 1,056 cm^{-1} (Si–O–Si) peak arose owing to the existence of Si–O–Si group. A 1,021 cm^{-1} enhanced due to the formation of Si–O–C groups [23]. Formation of the Si–O–C bonds favors compatibility between the organic and the inorganic phases [17]. The band at 995 cm^{-1} due to the stretching vibration of Si–OH could also be observed.

By comparing modified with that of unmodified SiO_2 (5%) nanocomposite membrane, it is clearly displayed that Si–O–Si stretching vibrations around 1,056 cm^{-1} boost up. But the strengthening of the relative intensity of the O–H bands was observed, indicating the residual silanol groups generated from hydrolysis reaction of the modified SiO_2.

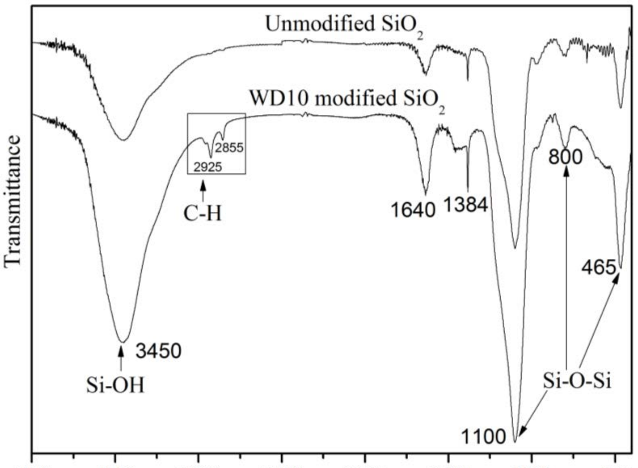

Fig. 1. FTIR spectra of nano-SiO_2 and WD10-modified SiO_2.

Moreover, in the presence of WD10, the loss of the 3,330 cm^{-1} peak intensity by adding the silane coupling reagent was observed, although the decrease in the peak intensity was very small. This strongly indicates the crosslinking reactions of WD10 with the cellulose membrane.

3.2.2. AFM analysis

AFM is an effective tool to characterize the membrane surfaces by providing the topography information. Fig. 4 shows the AFM images of the RC–SiO_2 (5%)-WD10 membrane with surface roughness (4 μm × 4 μm): R_a^a(nm) = 23.503; R_{ms}^b (nm) = 27.946. A quantification of the surface parameters provides an insight into morphological particularities which influence both the membrane separation properties and the process of modification. The surface roughness of these membranes gradually becomes smoother and denser as the SiO_2 content in the membrane matrix. These results indicate that cellulose is a hydrophilic polymer in nature and contains hydroxyl groups. The hydroxyl groups in the repeating units of the polymer are expected to produce strong interactions with the residual silanol groups of SiO_2, which facilitated a strong interfacial interaction [15]. So the compatibility between the organic and the inorganic phases is improved. Furthermore, the ridges of the nanocomposite membrane may be filled with SiO_2.

3.2.3. SEM analysis

Fig. 5 shows the SEM and AFM images of the top surface and cross-section of the pure RC and its nano-SiO_2 filled nanocomposite membranes. From Fig. 5(a), the thickness of membrane was found to be about 30–40 μm. From Figs. 5(b)–(d), the nonporous structure of dense membrane is observed from the surface views. No phase separation can be observed from the surfaces of the RC-SiO_2 and RC-SiO_2-WD10 membranes, indicating that these membranes are homogeneous in nature. While the bulges are observed from the surface morphology of RC-modified SiO_2, which suggests that the WD10 modified SiO_2 particles formed on the surface due to the modified SiO_2 conglomeration. So the surface roughness of the RC-modified SiO_2 membrane increased. Moreover, as shown in AFM (Figs. 5(e)–(g)), no pores and voids can be seen. It was considered that SiO_2 nanoparticles might have hydrophilic surface properties, resulting in high compatibility with cellulose membrane, due to the presence of silanol groups on the surface. While the hydrophilic surface properties of WD10-modified SiO_2 might reduce, resulting in low compatibility with RC membrane [24].

3.2.4. Thermogravimetric analysis

The thermal stability and decomposition behavior of RC-0 and RC-SiO_2 nanocomposite membranes were investigated by thermogravimetric analysis (TGA) under nitrogen

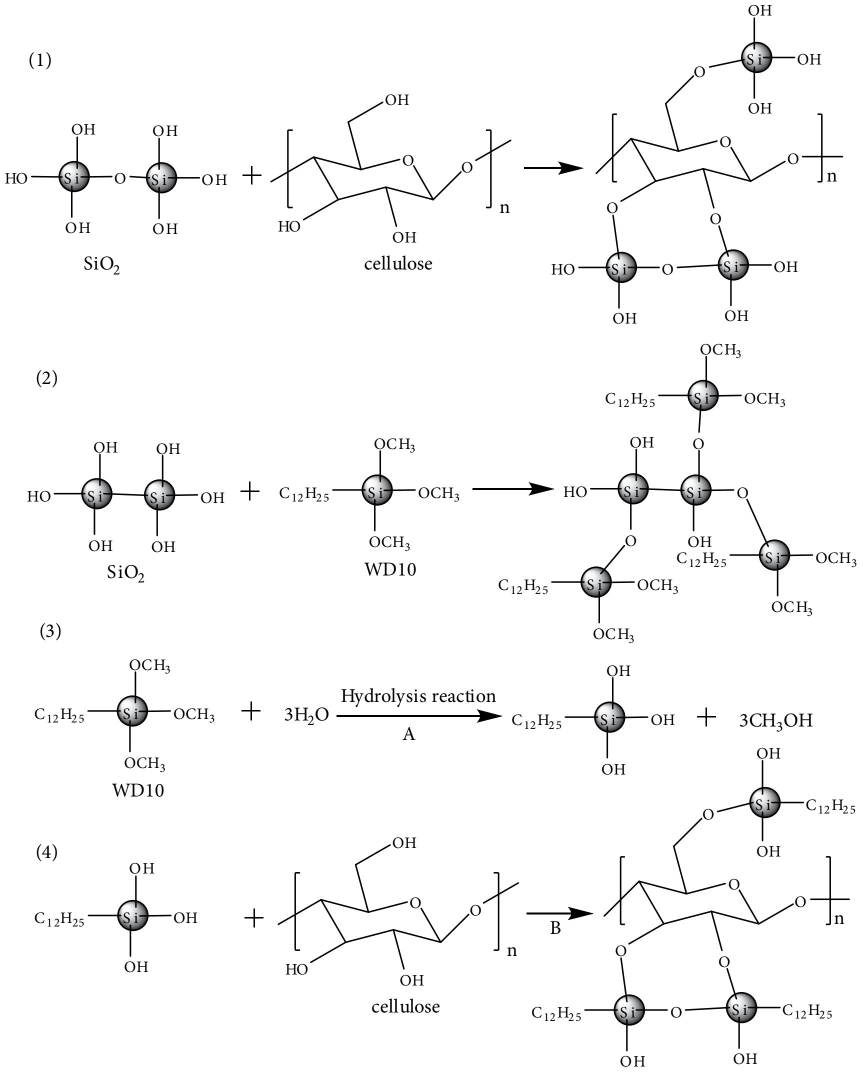

Fig. 2. Interaction of cellulose with SiO_2, SiO_2-modified with WD10, the crosslinking mechanism of cellulose with WD10.

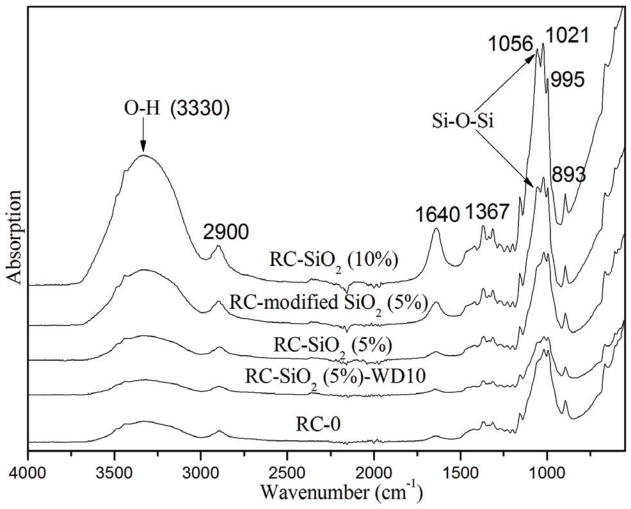

Fig. 3. ATR-FTIR of pure RC membrane, RC-unmodified SiO_2 or modified SiO_2 nanocomposite membranes.

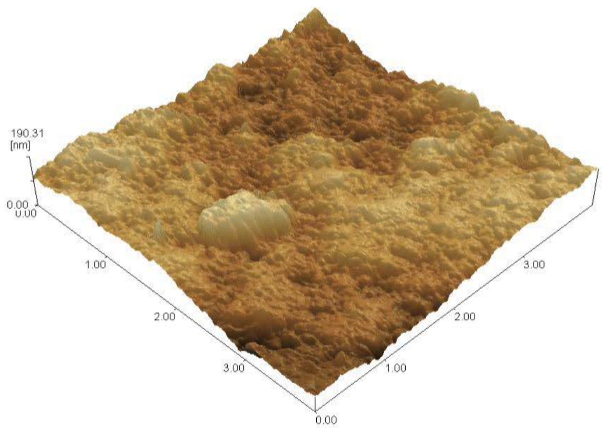

Fig. 4. 3D AFM topographic images of the RC-SiO_2(5%)-WD10 with surface roughness (4 µm × 4 µm): R_a^a(nm) = 23.503; R^b_{ms}(nm) = 27.946.

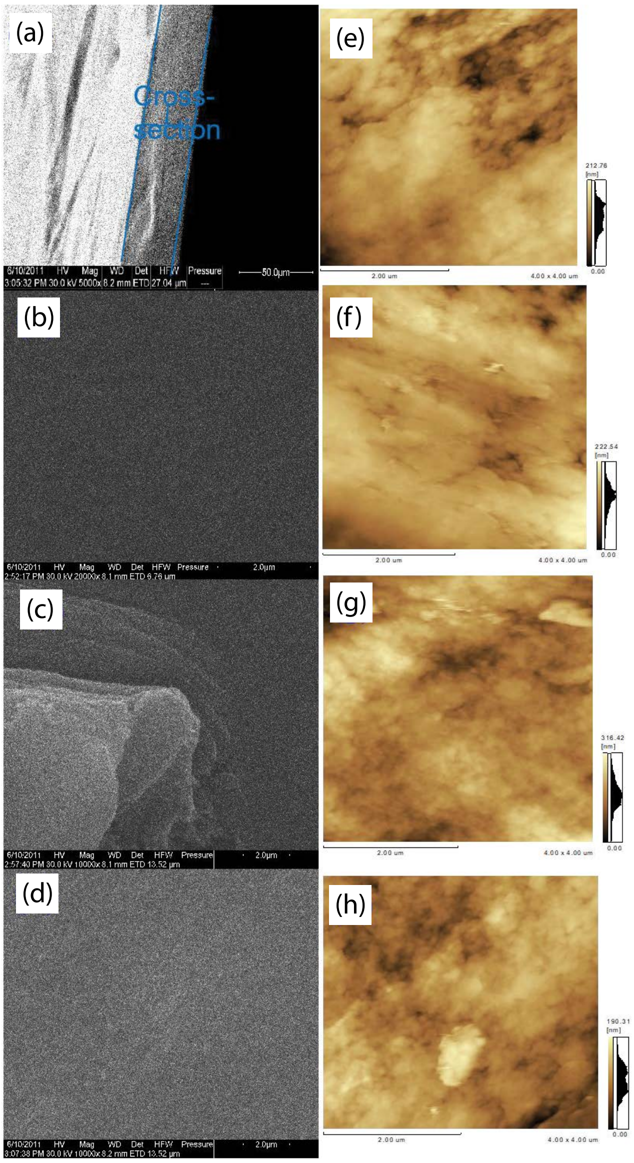

Fig. 5. SEM and 2D AFM photographs of the surface and cross-section of (a,e) RC-0, (b,f) RC-SiO_2(5%), (c,g) RC-modified SiO_2(5%, and (d,h) RC-SiO_2(5%)-WD10.

atmosphere, and the TGA curves are presented in Fig. 6. It can be seen that the nanocomposite membranes exhibit higher thermal stabilities with increasing SiO_2 content. The initial decomposition temperature increased from 250°C for the pure RC membrane to 266°C for the RC-modified SiO_2 (5%) membrane and 276°C for the RC-SiO_2 (5%) membrane. The increase of thermal stability could be attributed to the incorporation of SiO_2 since the presence of SiO_2 helped to absorb the thermal energy and thus protected RC membrane from thermal attack [19]. While the higher decomposition temperature of the RC-unmodified SiO_2 membrane than the RC-modified SiO_2 membrane could be due to the enhanced interaction between the unmodified SiO_2 and cellulose via hydrogen bonds. The thermal stability of RC-SiO_2-WD10 membrane was lowered by the addition of the coupling agent because of the alkyl chains of WD10.

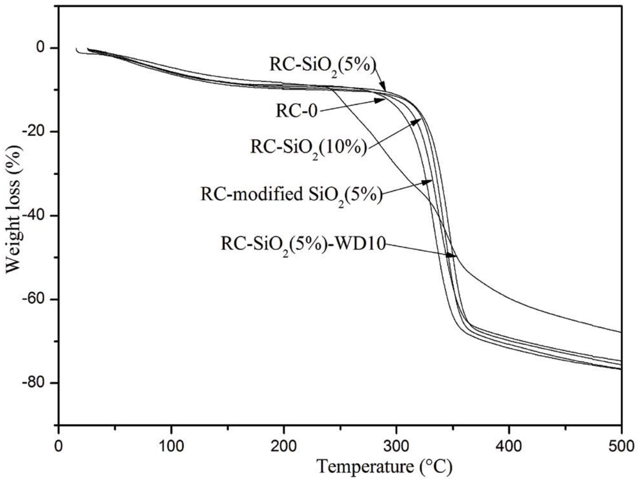

Fig. 6. TGA thermograms of RC-0 and RC-nanocomposite membranes.

3.2.5. XRD analysis

Fig. 7 presents XRD patterns of RC-SiO_2 nanocomposite membranes along with pure RC membrane and nano-SiO_2 powders. Clearly, the result of XRD analysis indicates that the SiO_2 nanoparticles are amorphous [25]. The diffraction peaks are observed at $2\theta = 12.0°$ and 22.5° for RC-0 membrane [26]. Compared with the pure RC membrane, the XRD patterns of nanocomposites show a little lower angle peak, at about $2\theta = 12°$. The RC-modified SiO_2 (5%) had the same characteristic peaks as the RC-unmodified SiO_2 (5%), suggesting that the crystalline structure of membranes was not changed with the same content SiO_2 and SiO_2 after WD10 modification. But the diffraction peaks of the RC-SiO_2-WD10 by adding the coupling agent directly show lowest percentage of crystallinity. These indicate that interaction occurred between cellulose and WD10.

3.3. Degree of swelling

Table 2 shows the degree of swelling of the RC nanocomposite membranes in the caprolactam–water mixtures under various water contents at 40°C. The swelling degree of RC-SiO_2 (10%) was slightly higher than RC-SiO_2 (5%). This indicates that the incorporation of hydrophilic SiO_2 nanoparticles is an effective approach of increasing the surface of the –OH groups. These –OH groups provide sites for hydrogen bonding between the polymer and water. Furthermore, when more SiO_2 nanoparticles were incorporated into the membrane matrix, it is likely that the pores of the membranes been occupied by the SiO_2 particles. This leads to an increased degree of swelling over that of the pure RC membrane [27]. The degree of swelling of RC-modified SiO_2 slightly decreased by the modification, indicating that the modified SiO_2 becomes more hydrophobic. The swelling degree decreased from RC-SiO_2(5%) to RC-SiO_2(5%)-WD10. The reason for this is that, the crosslinking network increased due to the hydrogen bonds which are formed between coupling silane agent and cellulose chains [17].

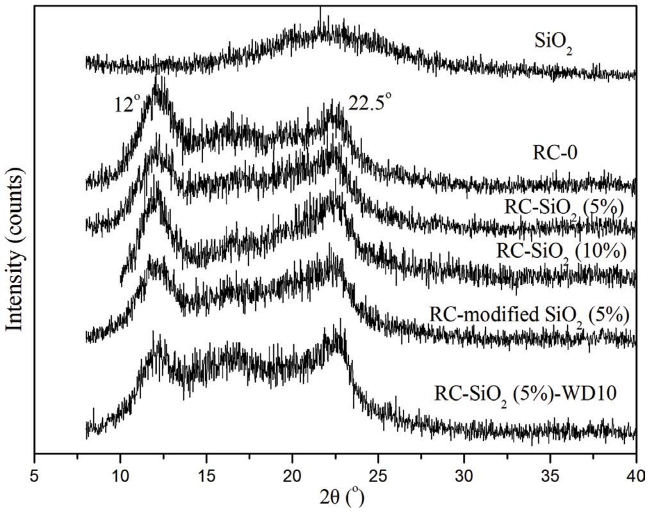

Fig. 7. XRD of pure SiO_2, RC-0 membrane, RC-nanocomposite membranes.

For all the nanocomposite membranes, the degree of swelling increased with increasing water concentration in the feed. Such swelling behavior indicates that the membranes are preferential to water which mainly arises from the interactions between water molecules and the –OH pendant groups of nanocomposite membranes [28].

3.4. PV performance results

3.4.1. Effect of membranes and feed temperature on PV performance

Fig. 8 shows the permeation flux and the separation factor at 70 wt.% caprolactam of unfilled RC and filled RC membranes as a function of the feed temperature. From Fig. 8(a), it is observed that for the same feed temperature RC-SiO_2(5%)-WD10 nanocomposite membrane exhibited both excellent flux and separation factor with a flux of 611.3 g m^{-2} h^{-1} and separation factor of 95,404.8 at 333 K. With crosslinking with WD10 and SiO_2 incorporation, the crystallinity of RC membrane is reduced as evident from XRD pattern (Fig. 7). The physical properties and PV performance were improved by crosslinking and organic–inorganic nanocomposite structure. Moreover, the introduction of the SiO_2 nanoparticles into the RC membrane would bring about extra free volumes in the polymer domains to increase the permeance rate of the membrane in PV dehydration [29].

The effects of SiO_2 and coupling silane agent modified SiO_2 fillers on the pervaporation properties of RC dense membranes have been studied. From Figs. 8(a) and (b), compared with the unfilled RC membrane, the filled RC membranes exhibited higher membrane PV performances. The SiO_2 nanoparticles might provide extra free volumes to offer spaces for water molecules to permeate through the membranes. Fig. 8(b) shows that the separation factor reveals decreasing trend with the rising temperature. But all the membranes have the excellent separation factor for the dense membrane with the slight increase of swelling of the membrane matrix.

The total flux and separation factor from the present study (for 50 wt.% caprolactam at 50°C, 55°C were compared with other composite membranes reported in literatures and presented in Table 3. Although the membranes are made from different material and preparation techniques, the dehydration performance of the RC-SiO_2 (5%)-WD10 composite membrane prepared in this study shows a comparable, good separation factor.

3.4.2. Effect of feed composition on PV performance

The effect of the feed concentration on the pervaporation performances is shown in Fig. 9, for concentrations of 30–60 wt.% of water in the feed mixtures. Figs. 9(a) and (b) show that the permeances of both water and caprolactam increase with increasing water feed concentration. This implies the highly hydrophilic cellulose membrane material, resulting in the higher degree of swelling (Fig. 7). The sorption of the membrane increases with increasing amounts of water. It is interesting that caprolactam permeance also increases. This increase of caprolactam permeance with water feed concentration reveals a coupling effect between caprolactam and water permeation through the membrane. So the membrane selectivity values (Fig. 9(c)) decreased considerably.

3.5. Diffusion coefficient

The transport of binary liquid molecules through a polymer membrane in PV process is generally described by the solution–diffusion mechanism, which occurs in three steps: sorption, diffusion and evaporation [30].

Diffusion coefficient is an important factor to understand the transport across the barrier membrane during pervaporation. Based on Fick's theory of diffusion, the diffusion coefficient can be calculated from the equation [23] as follows:

$$D_i = \frac{J_i \delta}{C_i} \tag{7}$$

Table 2
Degree of swelling data of membranes

Membrane	RC-0	RC-SiO_2 (5%)	RC-SiO_2 (10%)	RC-modified SiO_2 (5%)	RC-SiO_2 (5%)-WD10
30 wt.% caprolactam	54.85	56.72	57.64	55.09	55.22
50 wt.% caprolactam	52.38	52.43	54.33	53.81	52.63
70 wt.% caprolactam	50.96	51.92	53.26	52.63	51.88

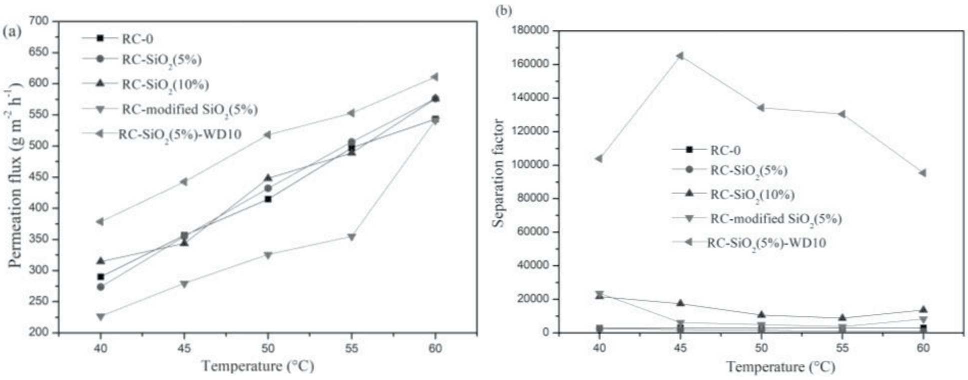

Fig. 8. Effect of the feed temperature on the pervaporation performances through different RC-nanocomposite membranes at 70 wt.% caprolactam aqueous solution: (a) permeation flux and (b) separation factor.

Table 3
Comparison of membrane separation performance with literatures

Membranes	Thickness (± μm)	Caprolactam in feed (wt.%)	Temperature (°C)	Total flux g m^{-2} h^{-1}	Separation factor	Reference
PVA cross-linked with 0.5 wt.% Gal	25–35	50	50	900	575	[6]
PVA/PAN composite membranes	80–100	50	55	1,802	890	[7]
PVA/PES composite membranes	110 ± 5	50	55	790	200	[8]
GA cross-linked NaAlg–PVP	80–100	50	50	1,634.4	1,610.6	[3]
composite membrane		50	55	2,220.5	1,354.7	
RC-5 membrane	40	50	55	1,787.3	55,091.7	[2]
RC-SiO$_2$(5%)-WD10	30–40	70	50	518.1	134,276.0	Present work

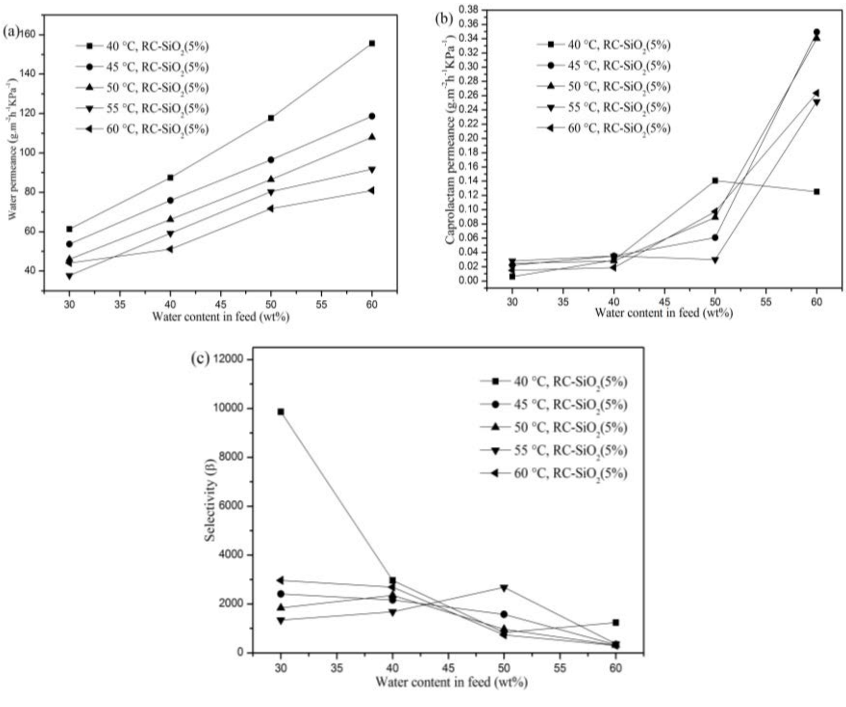

Fig. 9. Effect of the water content in feed on the pervaporation performances through RC-SiO$_2$(5%) membrane at different temperatures: (a) water permeance, (b) caprolactam permeance, and (c) selectivity.

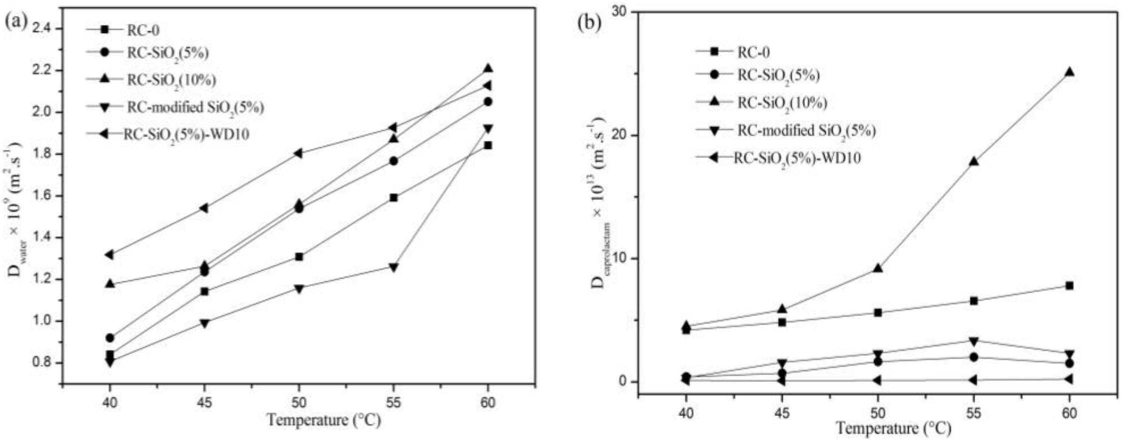

Fig. 10. Diffusion coefficients of water and caprolactam for different membranes calculated at different temperatures from Eq. (7) for 70 wt.% caprolactam in the feed.

where J_i, D_i and C_i are the permeation flux (g m^{-2}s^{-1}), diffusion coefficient (m^2 s^{-1}) and concentration of component i in the feed side of membranes (g m^{-3}), respectively. δ is membrane thickness (40 μm in this study).

Fig. 10 shows the diffusion coefficients of water (D_{water}) and caprolactam ($D_{caprolactam}$) through the nanocomposite membranes at temperatures between 40°C and 60°C. It is observed that D_{water} is much greater than $D_{caprolactam}$. This indicates that the RC and its nanocomposite membranes have the water-selective nature of the membranes. It is also found that diffusion coefficients of water as well as caprolactam increased systematically with increasing temperature, a trend that follows the conventional Arrhenius trend [12].

From Fig. 10(a), it is observed that for the same feed temperature the D_{water} shows the following trend:

$$\text{RC-SiO}_2\left(5\%\right)\text{-WD10} > \text{RC-SiO}_2\left(10\%\right) > \text{RC-SiO}_2\left(5\%\right) > \text{RC-0} > \text{RC-modified SiO}_2\left(5\%\right)$$

Also observed from Fig. 10(b), $D_{caprolactam}$ shows the following trend:

$$\text{RC-SiO}_2\left(10\%\right) > \text{RC-0} > \text{RC-modified SiO}_2\left(5\%\right) > \text{RC-SiO}_2\left(5\%\right) > \text{RC-SiO}_2\left(5\%\right)\text{-WD10}$$

Water diffusivities were found to be highest when the presence of WD10 is in the RC-SiO$_2$ (5%) nanocomposite membrane. As crosslinking with WD10 and SiO$_2$ incorporation, the crystallinity of RC-SiO$_2$(5%)-WD10 membrane is reduced, indicating a more flexible membrane structure and a higher water diffusion rate. A higher SiO$_2$ contents leads to a higher water diffusion rate. This was attributed to more hydrophilicity, selective adsorption and the establishment of molecular sieving action by the incorporation of SiO$_2$ inorganic material [30]. Compared with pure cellulose membrane, a decrease in diffusion coefficient of water for RC-modified SiO$_2$ (5%) could be due to a lower hydrophilic surface properties of WD10 modified SiO$_2$ and hence a reduced degree of swelling in the membrane, resulting in a reduced water diffusion rate [31]. The diffusion coefficients of both water and caprolactam for the nanocomposite membranes coincide with the permeance, indicating that the diffusion plays a dominant role in the transport of binary liquid molecules through a polymer membrane in PV process. The nanocomposite membranes developed in the present study have remarkable ability for the separation of caprolactam–water mixture, particularly, at higher temperature.

4. Conclusions

In this paper, novel organic–inorganic nanocomposite pervaporation membranes were prepared by the incorporation of the unmodified or a coupling silane agent (WD10)-modified SiO$_2$ into RC membranes. The WD10-modified SiO$_2$ particles were characterized by FTIR. Nanocomposite membranes were characterized by ATR-FTIR, AFM, SEM, TGA, XRD and degree of swelling techniques. Furthermore, these membranes were applied in caprolactam dehydration by pervaporation. The main conclusions are as follows:

- The FTIR spectrum indicates that the coupling agent WD10 was successfully grafted on the surface of SiO$_2$. The ATR-FTIR, AFM and SEM testing revealed that the unmodified SiO$_2$ nanoparticles had good dispersion and compatibility with the bio-polymer domain. But the WD10 modified SiO$_2$ nanoparticles dispersed on the surface and in the interior of the RC membranes due to the emergence of hydrophobicity group of $-C_{12}H_{25}$ on the surface SiO$_2$. XRD confirmed that crystallinity of nanocomposite membranes decreased, which benefited to enhance the membrane permeance. TGA illustrated that the nanocomposite membranes exhibit better thermal stability.
- The performance of the RC membrane was improved by the addition of inorganic particles. The RC-SiO$_2$-WD10 membrane exhibits both excellent permeation flux and separation factor. With crosslinking with WD10

and SiO_2 incorporation, the crystallinity of RC membrane is reduced as evident from XRD pattern. The physical properties and PV performance were improved by crosslinking and organic–inorganic nanocomposite structure.

- The diffusion coefficients of both water and caprolactam for the nanocomposite membranes coincide with the permeance, indicating that the diffusion plays a dominant role in the transport of binary liquid molecules through a polymer membrane in PV process. The nanocomposite membranes developed in the present study have remarkable ability for the separation of caprolactam–water mixture.

Symbols

J_i — Permeation flux of component *i*, g m^{-2} h^{-1}
J — Pervaporation permeation flux, g m^{-2} h^{-1}
D_i — Diffusion coefficient of component *i*, m^2 s^{-1}
S_i — Adsorption coefficient of component *i*, mol m^{-3} Pa^{-1}
δ — Membrane thickness, m
C_i — Concentration of component *i* in the feed, g m^{-3}
$p_{i,\text{feed}}$ — Vapor pressure of component *i* in feed, kPa
$p_{i,\text{permeate}}$ — Vapor pressure of component *i* in permeate, kPa
Q_i — Membrane permeance component *i*, g m^{-2} h^{-1} k^{-1}Pa^{-1}
T — Absolute temperature, K
A — Effective membrane area, m^2
W — Weight of penetrant, g
t — Permeation measuring time, h

Greek

β_{membrane} — Membrane selectivity
α — Pervaporation selectivity

Subscript

i — Component *i*, either water or caprolactam

References

[1] Q.G. Zhang, Q.L. Liu, Y. Chen, J.H. Chen, Dehydration of isopropanol by novel poly(vinyl alcohol)–silicone hybrid membranes, Ind. Eng. Chem. Res., 46 (2007) 913–920.

[2] T.R. Zhu, Y.W. Lin, Y.B. Luo, X. Hu, W.H. Lin, P. Yu, Preparation and characterization of TiO_2-regenerated cellulose inorganic–polymer hybrid membranes for dehydration of caprolactam, Carbohydr. Polym., 87 (2012) 901–909.

[3] T.R. Zhu, Y.B. Luo, Y.W. Lin, Study of pervaporation for dehydration of caprolactam through blend NaAlg-poly(vinyl pyrrolidone) membranes on PAN supports, Sep. Purif. Technol., 74 (2010) 242–252.

[4] V. Ragaini, C. Pirola, G. Rocco, C. Guaita, The beneficial influence of ultrasound in the polymerization of ε-caprolactam to polyamide-6 (Nylon 6). Part I: primary experimental results, Ultrason. Sonochem., 14 (2007) 680–688.

[5] M. Poschmann, J. Ulrich, Fractional suspension crystallization with additional purification steps, J. Cryst. Growth, 167 (1996) 248–252.

[6] L. Zhang, P. Yu, Y. Luo, Dehydration of caprolactam-water mixtures through cross–linked PVA composite pervaporation membranes, J. Membr. Sci., 306 (2007) 93–102.

[7] L. Zhang, P. Yu, Y.B. Luo, Separation of caprolactam–water system by pervaporation through cross-linked PVA membranes, Sep. Purif. Technol., 52 (2006) 77–83.

[8] L. Zhang, P. Yu, Y.B. Luo, Comparative behavior of PVA/PAN and PVA/PES composite pervaporation membranes in the pervaporative dehydration of caprolactam, J. Appl. Polym. Sci., 103 (2007) 4005–4011.

[9] J.H. Chen, Q.L. Liu, J. Fang, A.M. Zhu, Q.G. Zhang, Composite hybrid membrane of chitosan-silica in pervaporation separation of MeOH/DMC mixtures, J. Colloid Interface Sci., 316 (2007) 580–588.

[10] R. Fu, H.Z. Sai, L. Xing, J.H. Xiang, Z.Y. Li, T. Zhang, F.S. Zhang, Bacterial cellulose aerogels skeleton strengthened by regenerated cellulose, Key Eng. Mater., 697 (2016) 143–147.

[11] E. Nagy, O. Borlai, A. Ujhidy, Membrane permeation of water-alcohol binary mixtures, J. Membr. Sci., 7 (1980) 109–118.

[12] V.T. Magalad, G.S. Gokavi, K.V.S.N. Raju, T.M. Aminabhavi, Mixed matrix blend membranes of poly(vinyl alcohol)–poly(vinyl pyrrolidone) loaded with phosphomolybdic acid used in pervaporation dehydration of ethanol, J. Membr. Sci., 354 (2010) 150–161.

[13] V.T. Magalad, G.S. Gokavi, M.N. Nadagouda, T.M. Aminabhavi, Pervaporation separation of water–ethanol mixtures using organic–inorganic nanocomposite membranes, J. Phys. Chem. C, 115 (2011) 14731–14744.

[14] Z. Xie, M. Hoang, T. Duong, D. Ng, B. Dao, S. Gray, Sol-gel derived poly(vinyl alcohol)/maleic acid/silica hybrid membrane for desalination by pervaporation, J. Membr. Sci., 383 (2011) 96–103.

[15] H. Zou, S. Wu, J. Shen, Polymer/silica nanocomposites: preparation, characterization, properties, and applications, Chem. Rev., 108 (2008) 3893–3957.

[16] F.C. Oliveira, A. Barros-Timmons, J.A. Lopes-da-Silva, Preparation and characterization of chitosan/SiO_2 composite films, J. Nanosci. Nanotechnol., 10 (2010) 2816–2825.

[17] S. Razavi, A. Sabetghadam, T. Mohammadi, Dehydration of isopropanol by PVA–APTEOS/TEOS nanocomposite membranes, Chem. Eng. Res. Des., 89 (2011) 148–155.

[18] S. Yu, X. Zuo, R. Bao, X. Xu, J. Wang, J. Xu, Effect of SiO_2 nanoparticle addition on the characteristics of a new organic-inorganic hybrid membrane, Polymer, 50 (2009) 553–559.

[19] H. Zhou, Y. Su, X. Chen, S. Yi, Y. Wan, Modification of silicalite-1 by vinyltrimethoxysilane (VTMS) and preparation of silicalite-1 filled polydimethylsiloxane (PDMS) hybrid pervaporation membranes, Sep. Purif. Technol., 75 (2010) 286–294.

[20] P. Peng, B. Shi, Y. Lan, Preparation of PDMS-silica nanocomposite membranes with silane coupling for recovering ethanol by pervaporation, Sep. Sci. Technol., 46 (2011) 420–427.

[21] Y. Song, J. Zhou, L. Zhang, X. Wu, Homogenous modification of cellulose with acrylamide in NaOH/urea aqueous solutions, Carbohydr. Polym., 73 (2008) 18–25.

[22] J.G. Wijmans, Letter to the Editor, J. Membr. Sci., 220 (2003) 1–3.

[23] Q.G. Zhang, Q.L. Liu, F.F. Shi, Y. Xiong, Structure and permeation of organic-inorganic hybrid membranes composed of poly(vinyl alcohol) and polysilisesquioxane, J. Mater. Chem., 18 (2008) 4646–4653.

[24] A.L. Ahmad, M.A. Majid, B.S. Ooi, Functionalized PSf/SiO_2 nanocomposite membrane for oil-in-water emulsion separation, Desalination, 268 (2011) 266–269.

[25] L. Du, J. Tan, K. Wang, Y. Lu, G. Luo, Controllable preparation of SiO_2 nanoparticles using a microfiltration membrane dispersion microreactor, Ind. Eng. Chem. Res., 50 (2011) 8536–8541.

[26] Z.M. Mao, Y.M. Cao, X.M. Jie, Dehydration of isopropanol-water mixtures using a novel cellulose membrane prepared from cellulose/N-methylmorpholine-N-oxide/H_2O solution, Sep. Purif. Technol., 72 (2010) 28–33.

[27] A.A. Kittur, S.M. Tambe, S.S. Kulkarni, M.Y. Kariduraganavar, Pervaporation separation of water–acetic acid mixtures through NaY zeolite-incorporated sodium alginate membranes, J. Appl. Polym. Sci., 94 (2010) 2101–2109.

[28] S. Khoonsap, S. Amnuaypanich, Mixed matrix membranes prepared from poly(vinyl alcohol) (PVA) incorporated with zeolite 4A-graft-poly(2-hydroxyethyl methacrylate) (zeolite-g-PHEMA) for the pervaporation dehydration of water–acetone mixtures, J. Membr. Sci., 367 (2011) 182–189.

[29] Y.L. Liu, C.Y. Hsu, Y.H. Su, J.Y. Lai, Chitosan-silica complex membranes from sulfonic acid functionalized silica nanoparticles for pervaporation dehydration of ethanol-water solutions, Biomacromolecules, 6 (2005) 368–373.

[30] S.S. Kulkarni, S.M. Tambe, A.A. Kittur, M.Y. Kariduraganavar, Preparation of novel composite membranes for the pervaporation separation of water-acetic acid mixtures, J. Membr. Sci., 285 (2006) 420–431.

[31] M.N. Hyder, R.Y.M. Huang, P. Chen, Effect of selective layer thickness on pervaporation of composite poly(vinyl alcohol)–poly(sulfone) membranes, J. Membr. Sci., 318 (2008) 387–396.